# Main Manuscript for

# Intracellular Mannanases Sustain Matrix Polysaccharide Biosynthesis

Talia Jacobson[1,2], Mair Edwards[1,2], Moni Qiande[2], Madalen Robert[2,3], Julia Moncrieff[2], Cătălin Voiniciuc[1,2,3,4*]

[1]Plant Molecular and Cellular Biology Graduate Program, University of Florida, Gainesville, FL 32609, USA

[2]Department of Horticultural Sciences, University of Florida, Gainesville, FL 32609, USA

[3] Independent Junior Research Group–Designer Glycans, Leibniz Institute of Plant Biochemistry, 06120 Halle (Saale), Germany

[4]University of Florida Genetics Institute, University of Florida, Gainesville, FL 32610, USA

* **Corresponding Author:** Cătălin Voiniciuc

**Email:** cvoiniciuc@ufl.edu

**Author Contributions:** TJ and CV designed the work, analyzed data and wrote the manuscript. TJ acquired most of the data, with additional contributions from ME, MQ and JM. MR and CV developed the MannanTrack yeast strain.

**Competing Interest Statement:** The authors declare no competing interest.

**Classification:** Biological Sciences, Biochemistry

**Keywords:** plant cell wall, hemicellulose, polysaccharide biosynthesis, glycosyl hydrolases, synthetic biology

**This PDF file includes:**

Main Text
Fig. 1 to 5

**Abstract**

The most ancient and ubiquitous hemicellulosic components in the plant cell wall are the β-1,4-linked mannans. Despite their prominent position in the hydrocolloid market and numerous applications as gelling agents in food, feed, biomedical, and bioenergy sector, how β-mannans are assembled and modified remains poorly understood. This greatly limits our ability to improve their structure in crops or microbial cell factories. Glycosyl hydrolases known as endo-β-mannanases (MANs) are the primary catalysts that mobilize mannans from the plant cell wall by cleaving internal β-1,4 glycosidic bonds. Here, we report that Arabidopsis *man2 man5* double mutants produce less β-mannan in the seed coat epidermis, rejecting the current dogma that *man* mutants should maintain or over accumulate Man-rich polymers. While the reduced mannan content could be partially restored through overexpression of a CELLULOSE SYNTHASE-LIKE A (CSLA) glucomannan synthase in the *man* double mutant, this impaired other seed mucilage polysaccharides. To characterize the functional relationship between CSLAs and MANs, we applied synthetic biology approaches in a modular yeast platform. MAN2 and MAN5 localized intracellularly and reduced the content of alkaline-insoluble polymers made by plant CSLAs. The beneficial of effects of MAN2 was abolished by mutating a single amino acid in its hydrolytic core. By tracking mannans using a newly developed probe and detecting elevated content of water-soluble polymers, we propose that MAN2/5 sustain hemicellulose production in the Golgi apparatus by cleaving insoluble mannan polymers into more hydrophilic molecules.

**Significance Statement**

Plant β-1,4-linked mannans are found in many cell walls and have widespread industrial applications. Our study challenges the prevailing view that β-mannanase (MAN) enzymes cleave extracellular polysaccharides by demonstrating that Arabidopsis *man2 man5* double mutants produce less β-mannan. Overexpression of a glucomannan synthase partially restored mannan content but disrupted the secretion of other seed polysaccharides. Using yeast synthetic biology, we reveal that MAN2 and MAN5 are intracellular hydrolases that reduce the accumulation of insoluble polymers to enhance hemicellulose solubility and promote secretion. This work provides biochemical insights into the functional interplay between CSLAs and MANs, shedding new light on hemicellulose biosynthesis and on historic bottlenecks to elevate mannan content in plants.

## Main Text

### Introduction

The biosynthesis and degradation of cell wall polysaccharides are two of the most important processes that define the composition of plant biomass, the most abundant reserve of carbon on Earth (1). Hemicelluloses along with cellulose microfibrils and pectin domains are the main classes of polysaccharides driving plant development and responses to unpredictable environmental stimuli. Modifications of hemicellulosic components radically alter the cell surface architecture and stress physiology (2). In addition to their biological roles, the applications of cell wall polysaccharides are vast and include widespread use in food, feed, materials, and energy sectors. Furthermore, there is an increasing need to engineer hemicellulosic fibers for a sustainable, circular bioeconomy: whether to capture carbon into recalcitrant polymers for long-term carbon storage, or to convert lignocellulosic biomass into cost-effective feedstocks for biomanufacturing (3).

Despite the vast ecological and industrial applications of plant cell wall polysaccharides and the long-standing aim to enhance the proportion of hexose-rich hemicelluloses in bioenergy crops has not been challenging to address. The content of β-mannan has yet to be elevated in plants through genetic engineering, and prior attempts in seeds led to severe metabolic perturbations (4). The *Arabidopsis thaliana* (hereafter Arabidopsis) seed coat epidermal cells offer an excellent genetic model system to untangle how various carbohydrate-active enzymes impact cell wall polysaccharide structure and function. Upon contact with water, dry seeds release copious amounts of mucilage, a specialized cell wall (5), containing mixture of hydrophilic polysaccharides with smaller amounts of hemicelluloses such as branched β-mannans (6) and crystalline cellulose (7). Seed-extracted galactomannans (e.g. guar gum and locust bean gum) are frequently added as thickening agents, stabilizers and emulsifiers in numerous foods and household products, or serve as dietary fiber supplements to control appetite and reduce blood glucose (Glc) levels in patients with type 2 diabetes mellitus (8). In Arabidopsis mucilage, highly branched galactoglucomannan (GGM) contributes to mucilage density and crystalline cellulose deposition (6), while another hemicellulose, branched xylan, is important for the adherence of pectin (with rhamnogalacturonan I making up the bulk of mucilage) to the seed surface (9, 10). Plant β-mannans are defined by their β-1,4-linked mannose (Man) units, but can also contain β-1,4-Glc in their backbone. In Arabidopsis mucilage GGM, the Man units are substituted with single α-1,6-linked galactosyl (Gal) units (11, 12), or β-1,2-Gal-α-1,6-Gal disaccharides (11, 13).

As recently reviewed (3), β-mannan biosynthesis is orchestrated by several classes of Golgi-localized glycosyl transferase (GTs) with a suite of secreted glycosyl hydrolases (GHs) expected to modify polysaccharides after they are deposited in the cell wall. CELLULOSE SYNTHASE-LIKE A2 (AtCSLA2) is the chief catalyst for β-mannan elongation in the Arabidopsis seed coat (14). Based on orthogonal experiments in the yeast *Pichia pastoris*, AtCSLA2 works in partnership with the MANNAN-SYNTHESIS RELATED1 (MSR1) protein co-factor to incorporate both Glc and Man subunits in glucomannan (15). Functional characterization of CSLAs from several plants (including *Amorphophallus konjac* AkCSLA3 and *Coffea canephora* CcMANS1) in *Pichia* cells revealed distinct preference for Glc incorporation with or without MSR1. MUCILAGE-RELATED10 (MUCI10), also known as MAGT1 (12), decorates Man residues with Gal side chains (6) that are important for hydrophilicity. In contrast, other seeds such as palm nuts accumulate unbranched β-mannan polymers with crystalline properties (16) and serve as vegetable ivory to carve jewelry and other products. Nevertheless, how plant cells accumulate these unbranched polymers remains unclear, since *in vitro* assays show that mannan oligosaccharides crystallize as they elongate (17).

Here, we explore the biochemical and cellular roles of *MAN2* and *MAN5*, two *endo-β-1,4-MANNANASE* genes that are co-expressed in the Arabidopsis seed coat during mucilage production. As the chief enzymes for mannan bioconversion and transglycosylation, different MANs have been involved in seed germination, xylem development, floral organ formation, fruit ripening, silique dehiscence, and heavy metal tolerance (18–24). Since MANs are typically defined as hydrolytic enzymes, we hypothesized that *man2/5* single or double mutants would hyperaccumulate β-mannan polymers. Contrary to our initial expectations and the prevailing theory that MANs act in the extracellular space, we discovered that Arabidopsis *MAN2* and *MAN5* encode intracellular enzymes that are essential for β-mannan production in the seed coat epidermis. MAN2 and MAN5 also reduced the content of insoluble polymers and promoted secretion of a mannan-tracking probe in yeast cells bioengineered to accumulate hemicellulose.

## Results

### *man2 man5* Seeds Resemble Mannan-Deficient *csla2* and *muci10* Mutants

From seven MAN genes in Arabidopsis, four genes (MAN2, MAN5, MAN6, and MAN7) are expressed in germinating seeds (20), but their roles during seed coat development were unknown. We investigated how mucilage polysaccharides are affected by T-DNA mutations in *MAN2* and *MAN5* (Fig. 1A), since these genes are the closest paralogs and have partially overlapping expression during seed coat development (Fig. 1B). A *man2-1 man5-1* double mutant was obtained from the GABI-DUPLO collection (25), which generated targeted a number of unlinked gene pairs in Arabidopsis. Since GABI-DUPLO article did not report any obvious defects for the *man2 man5* seedlings or adult plants, we verified that these mutations reduced the transcript levels of the respective genes (Fig. 1C). While single and double mutant plants were morphologically indistinguishable from the Col-0 wild type (WT) at maturity, the *man2-1 man5-1* mucilage capsule was 30% more compact than WT (Fig. 1D and E) and resembled *csla2* and *muci10* mannan biosynthetic mutants (11). Since we could not verify the position of other insertions in *MAN5* (Table S1, we crossed an independent *man2-2* insertion (Fig. 1A), previously shown to be a transcriptional knockout (20), to *man5-1* plants and isolated a novel *man2-2 man5-1* double mutant through genotyping. The second mutant combination had a similar decrease in the mucilage area to *man2-1 man5-1* (Fig. 1D and E). Therefore, the *man2-1 man5-1* mutant was used as a representative background to test cloned genes (Table S2) in later experiments. In contrast to the mucilage defects, there were no obvious differences in seed area for the single or double mutants examined (Fig. 1D and E). The similarity between mutants affecting GTs and GHs, which should have opposite activities on mannan structure (Fig. 2A), prompted us to profile mucilage composition.

The matrix polysaccharides of total mucilage extractable with water (26) were profiled via high-performance anion-exchange chromatography with pulsed amperometric detection (HPAEC-PAD). While the *man2* and *man5* single mutants had a WT mucilage chemotype, both *man2 man5* double mutants accumulated significantly less Gal and Man, the most characteristic subunits of branched mannans (Fig. 2B; full profile in Table S3). Glc, the third component of GGM, generally had similar trends, but showed the highest coefficient of variation in the HPAEC-PAD results because it can be derived from unrelated polysaccharides, including starch. All other mucilage components, including rhamnose (Rha), galacturonic acid (GalA), arabinose (Ara), and xylose (Xyl), showed negligible changes between the genotypes, indicating that the compact mucilage results from reduced GGM accumulation. Across multiple growth batches (Fig. 2B, Fig. 2C and Fig. S1A), the *man2 man5* total mucilage chemotypes were nearly as severe as those of *csla2* and *muci10*, with up to 40 to 50% reductions in Gal and Man compared to WT. Therefore, rather than participating in mannan catabolism, *MAN2* and *MAN5* promote GGM biosynthesis in seeds.

### *AtCSLA2* Overexpression Rescues *csla2* Defects, but Impairs *man2 man5* Mucilage

We cloned *AtCSLA2* and *AtMAN2/5* cDNA sequences in Golden Gate-compatible vectors (Table S2) to characterize their functions in both plants and yeast (see last sections of the Results). Although CSLAs have been challenging to overexpress in plants, we discovered that the *TESTA ABUNDANT2* (*pTBA2),* a seed coat-specific promoter (27), enabled the AtCSLA2 cDNA sequence to rescue the *csla2* mannan deficiency (see plant construct summary in Table S4, and mucilage composition in Table S5). The transformation of *man2 man5* with *pTBA2*:*AtCSLA2* restored the absolute amounts of Man and Gal levels to almost WT levels, but decreased Rha and GalA content by nearly 60% (Fig. 2C) and further reduced mucilage capsule size (Fig. S2C). Unlike the reduced pectin content of the transformed *man2 man5* background, the *csla2* + *CSLA2* lines over accumulated Gal and Man but had WT-like levels of all other mucilage carbohydrates (Table S5). Scanning electron microscopy (SEM) of dry seeds did not reveal major changes in cell surface morphology, although the *man2 man5* seeds overexpressing *AtCSLA2* had slightly larger columellae (Fig. S1C). While seed immunolabeling with CCRC-M36 for rhamnogalacturonan I showed results consistent with ruthenium red staining, none of the three CCRC antibodies directed against mannans (28) were able to bind WT or *man2 man5* mucilage (Fig. S2A) so we turned our attention to a more general fluorescent stain for (hemi)cellulosic polysaccharides.

Calcofluor (CF) white staining revealed genotype-dependent changes in β-glucan distribution around the seed surface (Fig. 3A). While *csla2* mucilage had only faint CF fluorescence, *man2 man5* double mutant seeds displayed compact mucilage with an intermediate CF intensity compared to WT. The *pTBA2:AtCSLA2* transgene restored CF staining around *csla2* seeds but resulted in compact mucilage with wider, disordered rays in the *man2 man5* background (arrows in Fig. 3A). This trend was supported by the birefringence of crystalline polymers under polarized light, with *man* double mutants showing an intermediate reduction in birefringence compared to known mannan biosynthetic mutants (Fig. 3B, Fig. S1D). The *pTBA2:AtCSLA2* transgene increased birefringence compared to the respective mutant backgrounds, with *man2 man5* + CSLA approaching WT birefringence levels, and *csla2* + *CSLA2* exceeding them (Fig. S2B).

We also explored the physiological consequences of impaired GGM accumulation in the seeds. MAN activity is known to increase during seed germination in multiple species and the *man5-1* single mutant was previously shown to delay germination rate, while *man2-2* resembled the WT (20). We monitored the germination of WT, *csla2*, and our two *man2 man5* double mutant combinations for 5 days after stratification. By 72 h, *man2 man5* double mutants as well as *csla2* had only 50% germination in contrast to 90% of WT seeds. However, after an additional 48 h, the mutant genotypes also reached almost 100% germination (Fig. 3C). This suggests a functional interplay between AtMAN2/5 and AtCSLA2, which co-localized with a Golgi marker when transiently expressed in tobacco leaf epidermal cells (14).

**AtMAN2 is localized in intracellular compartments *in planta***

Although *pTBA2:AtCSLA2*$^{cDNA}$ stable transformants were clearly active in Arabidopsis, the *pTBA2:AtMAN*$^{cDNA}$ constructs did not rescue *man2 man5* staining or monosaccharide composition (Fig. 2C). As implied by its name and prior data (27), *pTBA2* is one of the strongest promoters for Arabidopsis seed coat epidermal cells. Concerned that *pTBA2* may be too strong, we cloned the putative *pMAN2* promoter, but *AtMAN2*$^{cDNA}$*-mCherry* still did not function in seeds (Fig. S1A). To test if the cDNA sequences codon-optimized for *Pichia pastoris* were responsible for poor expression in plants, *AtMAN2*$^{cDNA}$*-mCherry* was reassembled with the constitutive *Cauliflower Mosaic Virus 35S* promoter (*p35S*) for transient protein localization assays in *Nicotiana benthamiana* leaves. Unlike canonical MAN enzymes from plants and microbes, we noticed that AtMAN2 and AtMAN5 are predicted to have an N-terminal transmembrane domain rather than a signal peptide for extracellular secretion (Fig. 2A). Despite strong cytosolic expression for *p35S*-driven mCherry control (Fig. S1B), *AtMAN*$^{cDNA}$*-mCherry* lines showed no detectable fluorescence. Since *AtMAN*$^{cDNA}$ constructs showed no detectable fluorescence in

plants (summarized in Table S4) despite the yeast activities described in next section, we amplified their genomic sequences (gDNA) for fusions with mCherry driven by the Arabidopsis *UBIQUITIN10* promoter (*pUBQ10*). Although AtMAN5 remained undetectable in *N. benthamiana* leaves, AtMAN2$^{gDNA}$-mCherry localized in small punctae, reminiscent of the Golgi bodies (Fig. 3D).

**AtMAN2/5 Enzymes Reduce the Amount of Insoluble Mannans in *Pichia* CSLA strains**

To further investigate the biochemical effects of *MAN2* and *MAN5* on (gluco)mannan biosynthesis, we transformed *Pichia* CSLA strains (15) with additional transgenes under the control of different methanol-inducible promoters (Table S6). While plant *CSLA* genes were integrated into the *Pichia* genome, *MAN$^{cDNA}$-mCherry* constructs were introduced through an Plant MoClo-compatible episomal expression vector (29). After growth under selective pressure and methanol induction, alkaline-insoluble (AKI) yeast polymers were profiled via HPAEC-PAD. As previously reported (15), AkCSLA3 and AtCSLA2 produce glucomannan and relatively pure mannan in the AKI fraction (Fig. 4A). As a positive control, *AtMSR1* co-expression via the episomal vector in the *AkCSLA3* strain boosted glucomannan production by 10-15%, and enabled *AtCSLA2* to incorporate Glc into AKI polymers (Fig. 4A and Fig. S5A). In contrast, the co-expression of *MAN2* or *MAN5* with either AkCSLA3 or AtCSLA2 reduced the content of insoluble β-mannans by around 40% (Fig. 4A and Fig. S5A). AtMAN proteins localized in intracellular compartments (Fig. S3D) and did not alter the native yeast polymers in the X-33 control (Fig. 4A). To confirm that GH activity reduced the accumulation of insoluble hemicellulose, a single amino acid change (E335A; see Fig. S3) was introduced in the AtMAN2 glutamate residue corresponding to the catalytic nucleophile of plant and bacterial MANs (30). Despite similar fluorescence intensity and subcellular localization to the reference protein (Fig. S3D), AtMAN2$^{E335A}$ no longer altered (gluco)mannan production by CSLAs (Fig. 4A and Fig. S4A), consistent with the inability of the mutated protein to cleave β-1,4-Man bonds.

In addition to the episomal vector whose strong *pCAT1* promoter can be induced by glycerol depletion (31), we found similar effects on insoluble β-mannan accumulation in yeast using integrative *AtMAN-mRuby* constructs driven by the weaker *pFDH1* promoter. To check if MAN co-expression elevated the content of alkaline-soluble polysaccharides, we isolated three different cell wall fractions after alkaline-treatment of *Pichia* cells, determined the dry weight of each fraction and analyzed them via HPAEC-PAD (Fig. S5). While biochemical differences were evident in the AKI fraction, with reductions in Man content when MANs were co-expressed with CSLAs, no significant changes were detected in the alkaline-soluble polymers that were further separated into alcohol-soluble and insoluble glycans. However, the higher amount of endogenous Man-rich glycans enriched in the last two fractions could be obscuring changes in the solubility of (gluco)mannans.

**AtMAN2 and AtMAN5 Do Not Act on Extracellular Mannans**

Since plant MANs are reported to have low catalytic activity (30) compared to microbial counterparts exploited for bioenergy applications (32), we tested the performance of a microbial *AaMAN5a* from the plant pathogen *Aspergillus aculeatus* in *Pichia*. While AtMAN2 reduced AKI Man levels in the AtCSLA2 background by 46%, the introduction of *AaMAN5a* resulted in a 66% decrease (Fig. 4C), resembling the WT composition. Moreover, we attempted to secrete AtMAN2 and AtMAN5 by replacing their first 34 and 33 amino acids (Fig. S3A), respectively, with an α-mating factor (MF). Surprisingly, neither X-33 nor CSLA strains could secrete αMF-MAN proteins (Fig. S4B) or alter their subcellular localization (Fig. S3D). AaMAN5a was known to break down extracellular mannans when expressed in *Saccharomyces cerevisiae*, so we tested if MAN-expressing yeast cell cultures and their supernatant could digest Azurine Cross Linked (AZCL) galactomannan. Minute amounts of a commercial MAN enzyme (Megazyme E-BMANN) were

sufficient to release blue-dyed mannan oligosaccharides (Fig. 4D). When N-terminally tagged with *Saccharomyces* α-galactosidase (αGal) signal peptide, AaMAN5a was secreted well and digested AZCL-galactomannan. In contrast, no blue dye release was observed for AtMAN2 and AtMAN5 with either αGal or αMF peptides (Fig. 4D), indicating lower activity and poor secretion.

### AtMAN2/5 Co-Localize with AkCSLA3 in Yeast but Cannot Rescue its Toxic Effects

We hypothesized that MANs may co-localize with CSLA enzymes in the endomembrane system. Indeed, AtMAN2 and AtMAN5 tagged with mCherry co-localized with AkCSLA3-Venus (Fig. 4B, Fig. S4B). The relative AkCSLA3-Venus fluorescence remained constant with either mCherry or MAN-mCherry, indicating changes in insoluble Man content were not due to altered CSLA expression (Fig. S4C). Although only a portion of CSLA cells showed detectable mCherry signals after three days of cultivation, this was likely due to episomal variation and still led to caused population-wide in insoluble hemicellulose accumulation. We expected changes in yeast cell ultrastructure following glucomannan production, but could not identify Golgi stacks or other subcellular defects in 3-day-old cells via transmission electron microscopy following two different fixation methods (Fig. S6). Since the direct induction of glucomannan production by AkCSLA3 is toxic to *Pichia* cells (33), we investigated if the addition of AtMAN2/5 could alleviate these growth defects (Fig. S7). When grown in methanol as a sole carbon source to accentuate the toxic effects, all AkCSLA3 + MAN strains still showed the reduced optical density observed for AkCSLA3 alone, while the production of relatively pure mannans in AtCSLA2 strains with or without MANs did not alter biomass accumulation. Therefore, despite the reduction of insoluble glucomannan, the AkCSLA3 + MAN strain could still produce carbohydrates that compete with resources needed for yeast cell division and expansion.

### AtMAN2/5 Enzymes Promote a MannanTrack-ing Probe's Secretion and Polymer Solubility

In a separate study, we exploited the binding specificity of carbohydrate binding modules (CBMs; 37) to develop a non-invasive probe that monitors the products of CSLA enzymes (Robert and Voiniciuc, manuscript in preparation). Our MannanTrack probe is designed to secrete a mannan-specific *Podospora anserina* CBM35a (35) tagged with mScarlet, while a cytosolic mTurquoise protein acts as an internal control (Fig. 5A). After *Pichia* genome integration and methanol induction, the mScarlet secretion rate was inversely proportional to insoluble mannan production by CSLA (Fig. 5A-C and Fig. S8). All the mScarlet-tagged MannanTrack was secreted from X-33 cells without hemicellulose. When paired with AkCSLA3-Venus, most of the mScarlet was retained in intracellular compartments where glucomannan synthesis occurs (Fig. 5A and Fig. S8). Plate reader measurements, confocal microscopy and flow cytometry demonstrated that *MAN2* and *MAN5* increased MannanTrack secretion by 20% relative to an empty vector control (Fig. 5A-C and Fig. S8), while $MAN2^{E335A}$ could not significantly boost secretion. The increased secretion of MannanTrack prompted us to further investigate mannan solubility in *CSLA + MAN Pichia* strains. Following a method previously used to extract soluble β-glucans from yeast (36), we ground cells in ethanol and found no significant changes in the ethanol-soluble Man content of the examined genotypes (Fig. 5D). However, a subsequent extraction with hot water released significantly more Man from cells co-expressing AkCSLA3 and AtMAN2/5 (Fig. 5D) compared to AkCSLA3 alone or with the non-functional $MAN2^{E335A}$. Therefore, hydrophilic molecules were released from insoluble mannans through the intracellular, hydrolytic action of MAN enzymes in *Pichia* (Fig. 5D).

## Discussion

### You Can't Build a Wall Without Breaking a Few Bricks

Previously, plant MANs have been proposed to degrade or cut-and-paste β-mannan polysaccharides in the extracellular matrix (37–39). However, we found it peculiar that some *MANs* are co-expressed with *CSLAs* in seed transcriptomic datasets from crop species such as

coffee (40), despite the opposing biochemical consequences of GHs and GTs. In this study, we discovered that Arabidopsis *man2 man5* double mutants resemble the mucilage staining defects and composition of *csla2* and *muci10* seeds, deficient in glucomannan elongation and substitution with Gal residues (11, 14). The lower Gal and Man levels and reduced CF staining in *man2 man5* (Fig. 1E and Fig. 2B) indicate that mucilage accumulates fewer β-mannans without MAN2 and MAN5. Therefore, the seed coat epidermal cells seem to "close up shop" for mannan elongation in the Golgi apparatus rather than keep going in the absence of *MUCI10* or *MAN2/MAN5*.

While plant β-mannans can bind to cellulose (3, 17, 41) to form mechanical barriers, they also represent a carbon storage reservoir that can be mobilized to support seedling growth. Although we found that *MAN2* and *MAN5* encode the key GHs for intracellular mannan processing, we cannot exclude that an additional *MAN* might also participate in this process and/or could be up-regulated in *man2 man5* mutants. *MAN2*, *MAN5*, *MAN6* and *MAN7* are highly expressed during Arabidopsis seed germination and single mutants for all genes except for *man2,* have slower germination rates than WT (20). In our experiments, we found similar delays in germination for *csla2* and *man2 man5* double mutants (Fig. 3C), which we re-interpret as storing fewer mannans during seed development. When comparing the Arabidopsis homologs cataloged in the ARAMEMNON database (42), only MAN2 and MAN5 are consistently predicted to have transmembrane domains, supporting their non-canonical roles in cell wall synthesis.

**Hemicellulose Structure Is Paramount for Matrix Polysaccharide Secretion**

There is increasing evidence for the biosynthetic, structural and functional similarities between branched mannans and xyloglucans in plants (43). As reported for xyloglucan (44), we hypothesize that the elongation of unbranched mannans would be detrimental for their secretion to the cell wall, which is supported by our MannanTrack observations in yeast (Fig. 5), and could disrupt the production of other matrix polysaccharides. Although *AtCSLA2* overexpression in *man2 man5* restored Gal and Man content to nearly WT levels, mucilage release and pectin content was reduced (Fig. 2C and Fig. S2C). We propose a model that, in the absence of MAN2/5, *AtCSLA2* overexpression elongates partially substituted GGMs that aggregate in the endomembrane system and thus cannot reach the extracellular locations observed in WT seeds (Fig. 5E). Xyloglucan mutants lacking Gal decorations show intracellular polysaccharide aggregates (44). While it is unclear if any endo-glucanase acts like MAN2/5 on intracellular xyloglucan, our model is supported by a related mechanism for the regulation of crystalline cellulose biosynthesis. KORRIGAN1 is a plasma membrane-localized cellulase that is part of the Cellulose Synthase Complex and influences its movement and the deposition of microfibrils in the extracellular space (45). Therefore, the reduced content of water-extractable mucilage from *man2 man5* + *CSLA2* seeds could be due to (i) reduced secretion of rhamnogalacturonan I to the cell wall and/or (ii) impaired release/expansion of pectin due to the incorporation of more crystalline polymers showing birefringence. Both options are still open, since the SEM of dry seeds revealed relatively minor changes in columella appearance (Fig. S1C), in contrast to mutations in GTs required for rhamnogalacturonan I biosynthesis (46).

**Yeast to the Rescue: Unraveling CSLA and MAN Roles through Synthetic Biology**

How plants synthesize and modify mannan polysaccharides throughout development, to adapt to abiotic challenges such as drought, or to defend against pathogen attacks remains unclear. Arabidopsis MANs likely share similar biochemical activities but exhibit diverse biological functions. For example, AtMAN6 and AtMAN3 are reported to release signaling molecules that trigger secondary wall thickening in xylem or responses to heavy metals such as cadmium, respectively (22, 23). While *in vitro* GH assays can yield useful catalytic benchmarks(47), they would not have revealed the unexpected biological roles of AtMAN2 and AtMAN5. Therefore, orthogonal living systems can be ideal to decipher the cellular functions of carbohydrate-active enzymes (48). By transforming yeast strains previously engineered to accumulate plant β-mannans (15), we found that intracellular MAN2 and MAN5 enzymes reduced the accumulation of insoluble mannans through a variety of experiments (Fig. 4), including the application of a novel MannanTrack probe to quantify hemicellulose distribution in yeast (Fig. 5). Surprisingly,

even when replacing the transmembrane domain with αMF or αGal secretion signals that work for MannanTrack and the microbial AaMAN5a, respectively, yeast cells showed no evidence of AtMAN2/5 secretion. Although AtMAN2 was affinity purified from *Pichia* cultures for *in vitro* assays using a similar N-terminal truncation (30), there are some differences in the recombinant protein tags as well as our use of the stronger *pCAT1* promoter in the episomal vectors (31). Nevertheless, additional amino acid motifs or interactions with membrane-anchored proteins could be responsible for the intracellular retention of AtMAN2/5.

MAN hydrolytic activity was important for the effects observed in yeast because the E335A mutation abolished the impact of AtMAN2 on mannan production (Fig. 4A, Fig. 5) despite not altering its expression level or localization (Fig. S3 and S8). Moreover, CSLA + MAN genotypes with a lower AKI Man content had an increase in water-soluble Man (Fig. 5E), which could represent mannan oligosaccharides. Using the same extraction method, *CELLULOSE SYNTHASE-LIKE C4* (*CSLC4*) expression in *Pichia* produced water-soluble β-1,4-linked glucan oligosaccharides with an estimated length of four to six residues (36), while co-expression with XXT1 (a xylosyltransferase enzyme belonging to the GT34 family that includes MUCI10) leads to the accumulation of more alkaline-insoluble glucans (33). We thus hypothesize that AkCSLA3 still has toxic effects even when co-expressed with AtMANs because soluble glucomannan accumulation may still compete with yeast glycans required for growth. Cells producing relatively pure β-mannan or β-glucans did not have this growth penalty (33), so future studies should test a broader range of CSLAs from across the plant kingdom to better understand which sequences lead to Glc and Man incorporation and the consequences of their products. In summary, the unexpected roles of plant MANs in CSLA-driven hemicellulose biosynthesis open up new paths to go glyco (49) and to valorize mannan fibers from plants for the bioeconomy.

## Materials and Methods

The MoClo Toolkit was a gift from Sylvestre Marillonnet (Addgene kit # 1000000044), the MoClo Plant Parts Kit was a gift from Nicola Patron (Addgene kit # 1000000047), and the GoldenPiCS Kit was a gift from the Gasser/Mattanovich/Sauer Group (Addgene kit #1000000133). Details regarding all plant and yeast experiments, including cultivation conditions, construct assembly, biochemical analyses, cytometry and microscopy are provided in the Supplemental Materials and Methods.

## Acknowledgments

We thank the following individuals for their technical assistance: Bo Yang (initial *man2 man5* screening), Hannah Zheng (seed phenotyping), and Karen Kelley (SEM and TEM sample preparation at the University of Florida ICBR Electron Microscopy Core Facility, RRID:SCR_019146). Sylvestre Marillonnet provided expert advice for MoClo design and assembly. We also thank Kristen Leach in Marcio Resende's lab for access to a real-time PCR machine. Doug Smith and Mariza Miranda provided excellent technical advice for confocal microscopy and flow cytometry at the University of Florida ICBR Cytometry Core Facility, RRID:SCR_019119. This work was supported by startup funding from UF/IFAS, the Horticultural Sciences Department, and the USDA National Institute of Food and Agriculture, Research Capacity Fund (Hatch) project 7004470 to C.V. In addition, T.J. and M.E. thank the PMCB program and College of Agricultural and Life Sciences (CALS) Dean's Awards for graduate research funding. The research visit of M.R. was supported by a DAAD (German Academic Exchange Service) scholarship, while J.M. was supported by the UF University Scholars program. Finally, we thank Toshihisa Kotake for helpful discussions about MAN function since learning about our independent approaches in the summer of 2024.

## References


1. Y. M. Bar-On, R. Phillips, R. Milo, The biomass distribution on Earth. *Proceedings of the National Academy of Sciences* **115**, 6506–6511 (2018).

2. B. Yang, F. Hofmann, B. Usadel, C. Voiniciuc, Seed hemicelluloses tailor mucilage properties and salt tolerance. *New Phytologist* **229**, 1946–1954 (2020).

3. C. Voiniciuc, Modern mannan: a hemicellulose's journey. *New Phytologist* **234**, 1175–1184 (2022).

4. M. Naoumkina, *et al.*, Metabolic and genetic perturbations accompany the modification of galactomannan in seeds of Medicago truncatula expressing mannan synthase from guar (Cyamopsis tetragonoloba L.). *Plant Biotechnology Journal* **6**, 619–631 (2008).

5. C. Voiniciuc, B. Yang, M. H.-W. Schmidt, M. Günl, B. Usadel, Starting to gel: how Arabidopsis seed coat epidermal cells produce specialized secondary cell walls. *International Journal of Molecular Sciences* **16**, 3452–3473 (2015).

6. C. Voiniciuc, *et al.*, MUCILAGE-RELATED10 Produces Galactoglucomannan That Maintains Pectin and Cellulose Architecture in Arabidopsis Seed Mucilage. *Plant Physiol.* **169**, 403–420 (2015).

7. J. S. Griffiths, *et al.*, Unidirectional Movement of Cellulose Synthase Complexes in Arabidopsis Seed Coat Epidermal Cells Deposit Cellulose Involved in Mucilage Extrusion, Adherence, and Ray Formation. *Plant Physiology* **168**, 502–520 (2015).

8. A. E. Juhász, *et al.*, Galactomannans are the most effective soluble dietary fibers in type 2 diabetes: a systematic review and network meta-analysis. *The American Journal of Clinical Nutrition* **117**, 266–277 (2023).

9. C. Voiniciuc, *et al.*, Highly Branched Xylan Made by IRREGULAR XYLEM14 and MUCILAGE-RELATED21 Links Mucilage to Arabidopsis Seeds. *Plant Physiology* **169**, 2481–95 (2015).

10. M.-C. Ralet, *et al.*, Xylans Provide the Structural Driving Force for Mucilage Adhesion to the Arabidopsis Seed Coat. *Plant Physiology* **171**, 165–178 (2016).

11. C. Voiniciuc, *et al.*, MUCILAGE-RELATED10 Produces Galactoglucomannan That Maintains Pectin and Cellulose Architecture in Arabidopsis Seed Mucilage. *Plant Physiology* **169**, 403–420 (2015).

12. L. Yu, *et al.*, The Patterned Structure of Galactoglucomannan Suggests It May Bind to Cellulose in Seed Mucilage. *Plant Physiology* **178**, 1011–1026 (2018).

13. L. Yu, *et al.*, Eudicot primary cell wall glucomannan is related in synthesis, structure and function to xyloglucan. *The Plant Cell* koac238 (2022). https://doi.org/10.1093/plcell/koac238.

14. L. Yu, *et al.*, CELLULOSE SYNTHASE-LIKE A2, a Glucomannan Synthase, Is Involved in Maintaining Adherent Mucilage Structure in Arabidopsis Seed. *Plant Physiol.* **164**, 1842–1856 (2014).

15. C. Voiniciuc, M. Dama, N. Gawenda, F. Stritt, M. Pauly, Mechanistic insights from plant heteromannan synthesis in yeast. *Proc. Natl. Acad. Sci. U.S.A.* **116**, 522–527 (2019).

16. H. Chanzy, M. Dube, R. H. Marchessault, J. F. Revol, Single crystals and oriented crystallization of ivory nut mannan. *Biopolymers* **18**, 887–898 (1979).

17. F. Grimaud, *et al.*, *In Vitro* Synthesis and Crystallization of β-1,4-Mannan. *Biomacromolecules* **20**, 846–853 (2019).

18. S. A. Filichkin, J. M. Leonard, A. Monteros, P.-P. Liu, H. Nonogaki, A Novel Endo-β-Mannanase Gene in Tomato LeMAN5 Is Associated with Anther and Pollen Development. *Plant Physiology* **134**, 1080–1087 (2004).

19. R. Schröder, T. F. Wegrzyn, N. N. Sharma, R. G. Atkinson, LeMAN4 endo-β-mannanase from ripe tomato fruit can act as a mannan transglycosylase or hydrolase. *Planta* **224**, 1091–1102 (2006).

20. R. Iglesias-Fernández, M. C. Rodríguez-Gacio, C. Barrero-Sicilia, P. Carbonero, A. Matilla, Three endo-β-mannanase genes expressed in the micropylar endosperm and in the radicle influence germination of Arabidopsis thaliana seeds. *Planta* **233**, 25–36 (2011).

21. Y. Zhao, D. Song, J. Sun, L. Li, *Populus* endo-beta-mannanase PtrMAN6 plays a role in coordinating cell wall remodeling with suppression of secondary wall thickening through generation of oligosaccharide signals. *Plant J* **74**, 473–485 (2013).

22. J. Chen, *et al.*, *MAN 3* gene regulates cadmium tolerance through the glutathione-dependent pathway in *Arabidopsis thaliana*. *New Phytologist* **205**, 570–582 (2015).

23. R. Zhang, B. Li, Y. Zhao, Y. Zhu, L. Li, An essential role for mannan degradation in both cell growth and secondary cell wall formation. *Journal of Experimental Botany* erad463 (2023). https://doi.org/10.1093/jxb/erad463.

24. H. He, *et al.*, CELLULASE6 and MANNANASE7 affect cell differentiation and silique dehiscence. *Plant Physiology* **176**, 2186–2201 (2018).

25. C. Bolle, *et al.*, GABI-DUPLO: a collection of double mutants to overcome genetic redundancy in Arabidopsis thaliana. *Plant J* **75**, 157–171 (2013).

26. C. Voiniciuc, M. Günl, Analysis of Monosaccharides in Total Mucilage Extractable from Arabidopsis Seeds. *BIO-PROTOCOL* **6**, 1–12 (2016).

27. R. McGee, *et al.*, Pectin Modification in Seed Coat Mucilage by *In Vivo* Expression of Rhamnogalacturonan-I- and Homogalacturonan-Degrading Enzymes. *Plant and Cell Physiology* **62**, 1912–1926 (2021).

28. K. Thorne, B. R. Urbanowicz, M. G. Hahn, “Plant Cell Wall Glycan-Directed Monoclonal Antibodies” in *Plant Cell Walls*, 1st Ed., (CRC Press, 2023), pp. 206–236.

29. P. Püllmann, *et al.*, A modular two yeast species secretion system for the production and preparative application of unspecific peroxygenases. *Commun Biol* **4**, 1–20 (2021).

30. Y. Wang, *et al.*, Biochemical characterization of the novel endo-β-mannanase AtMan5-2 from Arabidopsis thaliana. *Plant Science* **241**, 151–163 (2015).

31. T. Vogl, *et al.*, A Toolbox of Diverse Promoters Related to Methanol Utilization: Functionally Verified Parts for Heterologous Pathway Expression in Pichia pastoris. *ACS Synth. Biol.* **5**, 172–186 (2016).

32. J. Ishii, *et al.*, From mannan to bioethanol: cell surface co-display of β-mannanase and β-mannosidase on yeast Saccharomyces cerevisiae. *Biotechnol Biofuels* **9**, 188 (2016).

33. M. Robert, *et al.*, Modular biosynthesis of plant hemicellulose and its impact on yeast cells. *Biotechnol Biofuels* **14**, 140 (2021).

34. C. Voiniciuc, M. Pauly, B. Usadel, Monitoring polysaccharide dynamics in the plant cell wall. *Plant Physiology* **176**, 2590–2600 (2018).

35. M. Couturier, *et al.*, Structural and Biochemical Analyses of Glycoside Hydrolase Families 5 and 26 β-(1,4)-Mannanases from Podospora anserina Reveal Differences upon Manno-oligosaccharide Catalysis *. *Journal of Biological Chemistry* **288**, 14624–14635 (2013).

36. J.-C. Cocuron, *et al.*, A gene from the cellulose synthase-like C family encodes a β-1,4 glucan synthase. *Proc. Natl. Acad. Sci. USA* **104**, 8550–8555 (2007).

37. J. D. Bewley, Breaking down the walls — a role for endo-β-mannanase in release from seed dormancy? *Trends in Plant Science* **2**, 464–469 (1997).

38. L. R. S. Moreira, E. X. F. Filho, An overview of mannan structure and mannan-degrading enzyme systems. *Appl Microbiol Biotechnol* **79**, 165–178 (2008).

39. R. Schröder, R. G. Atkinson, R. J. Redgwell, Re-interpreting the role of endo-β-mannanases as mannan endotransglycosylase/hydrolases in the plant cell wall. *Annals of Botany* **104**, 197–204 (2009).

40. T. Joët, *et al.*, Regulation of galactomannan biosynthesis in coffee seeds. *Journal of Experimental Botany* **65**, 323–337 (2014).

41. A. Ebringerová, Z. Hromádková, T. Heinze, “Hemicellulose” in *Polysaccharides I*, Advances in Polymer Science., T. Heinze, Ed. (Springer-Verlag, 2005), pp. 1–67.

42. R. Schwacke, *et al.*, ARAMEMNON, a novel database for Arabidopsis integral membrane proteins. *Plant Physiol.* **131**, 16–26 (2003).

43. A. Grieß-Osowski, C. Voiniciuc, Branched mannan and xyloglucan as a dynamic duo in plant cell walls. *Cell Surf* **9**, 100098 (2023).

44. N. Hoffmann, H. E. McFarlane, Xyloglucan side chains enable polysaccharide secretion to the plant cell wall. *Developmental Cell* S1534580724003848 (2024). https://doi.org/10.1016/j.devcel.2024.06.006.

45. T. Vain, *et al.*, The Cellulase KORRIGAN Is Part of the Cellulose Synthase Complex. *Plant Physiology* **165**, 1521–1532 (2014).

46. C. Voiniciuc, *et al.*, Identification of Key Enzymes for Pectin Synthesis in Seed Mucilage. *Plant Physiology* **178**, 1045–1064 (2018).

47. T. Jacobson, M. Edwards, C. Voiniciuc, Sharp solutions to cleave plant fibers. *Current Opinion in Biotechnology* **90**, 103219 (2024).

48. M. Pauly, *et al.*, The Suitability of Orthogonal Hosts to Study Plant Cell Wall Biosynthesis. *Plants* **8**, 516 (2019).

49. C. Voiniciuc, It's time to go glyco in cell wall bioengineering. *Current Opinion in Plant Biology* **71**, 102313 (2023).

**Figures**

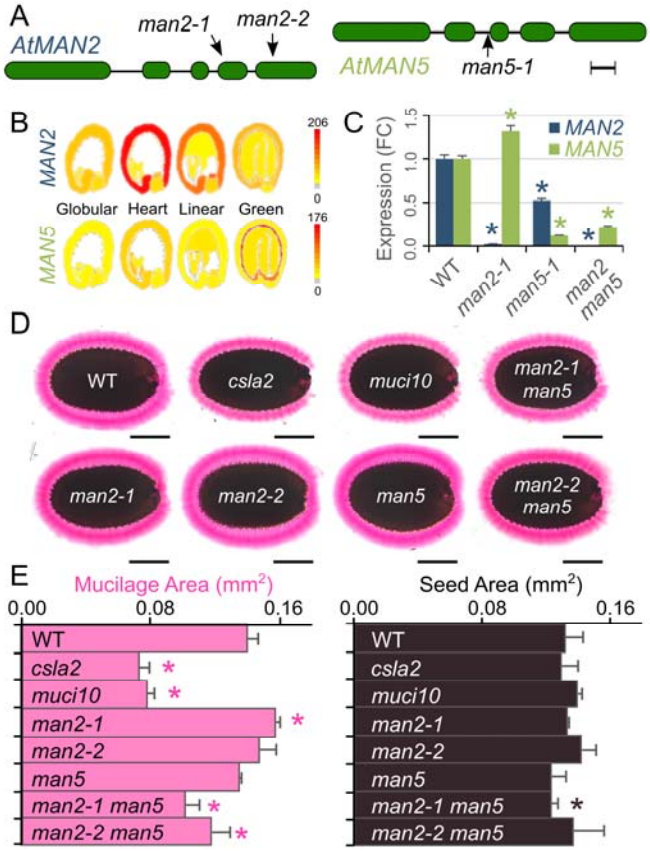


**Fig. 1.** Mannanase double mutants resemble Arabidopsis seeds with impaired β-mannan biosynthesis. *(A)* T-DNA insertions in *AtMAN2* and *AtMAN5* genes, showing exon and intron structure. (Scale bar, 200 bp). *(B)* Transcription profiles during seed development visualized with the eFP browser (50) *(C)* Fold change in *AtMAN2* and *AtMAN5* transcription relative to WT in mature green siliques. Bars show mean + SD of three biological replicates normalized to *UBIQUITIN5*. *(D)* Pectin release of WT and mutant seeds stained with RR. (Scale bars, 200 µm). *(E)* Projected surface area of mucilage and seeds. Data shows mean + SD of three biological replicates (around 20 seeds each). Asterisks in E panels indicate significant decreases relative to WT (Student's *t* test, $P < 0.05$).

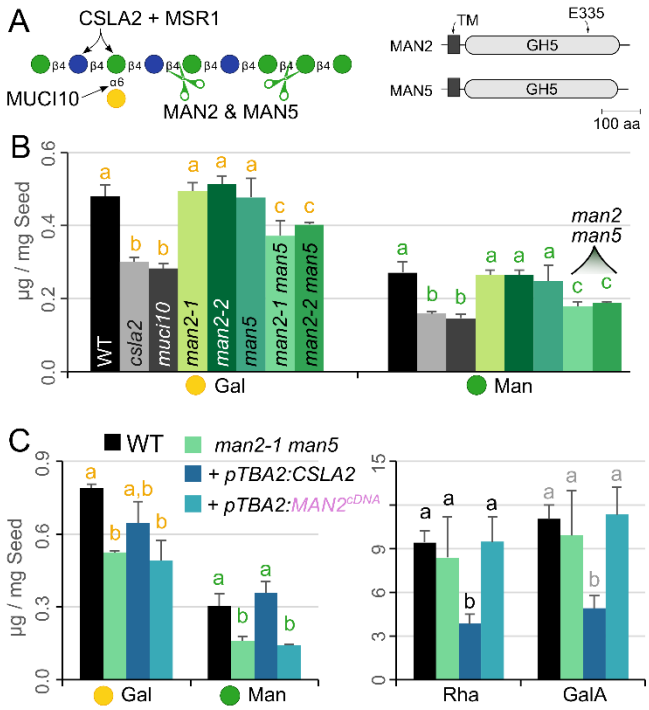


**Fig. 2.** The *man2 man5* mutant seeds impair β-mannan elongation by *AtCSLA2*. *(A)* Schematic of seed mucilage GGM structure and the predicted motifs of MAN2 and MAN5. Arrows indicate glycosidic bond formation and scissors indicate potential cut sites. *(B) man2 man5* double mutants have similar biochemical defects to *csla2* and *muci10.* Data shows mean + SD for the absolute monosaccharide levels of three biological replicates. *(C)* Overexpression of *AtCSLA2* in *man2 man5* restores Gal and Man content but decreases pectin release compared to WT. For each monosaccharide, different letters denote significant changes with one-way ANOVA (Tukey's post-hoc test, $P < 0.01$).

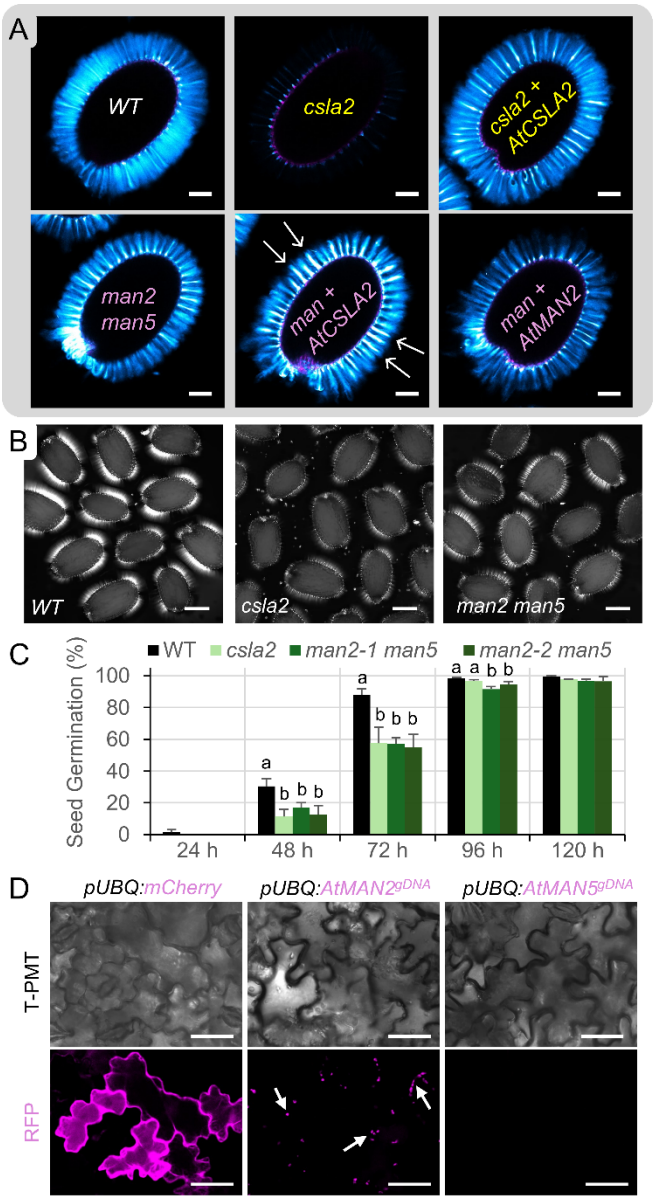


**Fig. 3.** Intracellular MAN enzymes are important for crystalline polymer structure and seed germination. (*A*) Calcofluor staining of β-glucans in seed mucilage. The mutants were transformed with cDNA sequences also used for yeast experiments. Arrows mark disordered rays not seen in other genotypes. (Scale bars, 100 µm) (*B*) Birefringence of crystalline polymers after seed hydration in water. (Scale bars, 200 µm). (*C*) Germination rates in water. Bars show mean + SD of three biological replicates. For each timepoint, different letters denote significant changes with one-way ANOVA (Tukey's post-hoc test, $P < 0.01$). (*D*) Optical sections of *Nicotiana benthamiana* leaves following infiltration with *pUBQ10*-driven expression for mCherry or MAN genomic sequences with mCherry tags. Arrows mark intracellular punctae. (Scale bars, 50 µm).

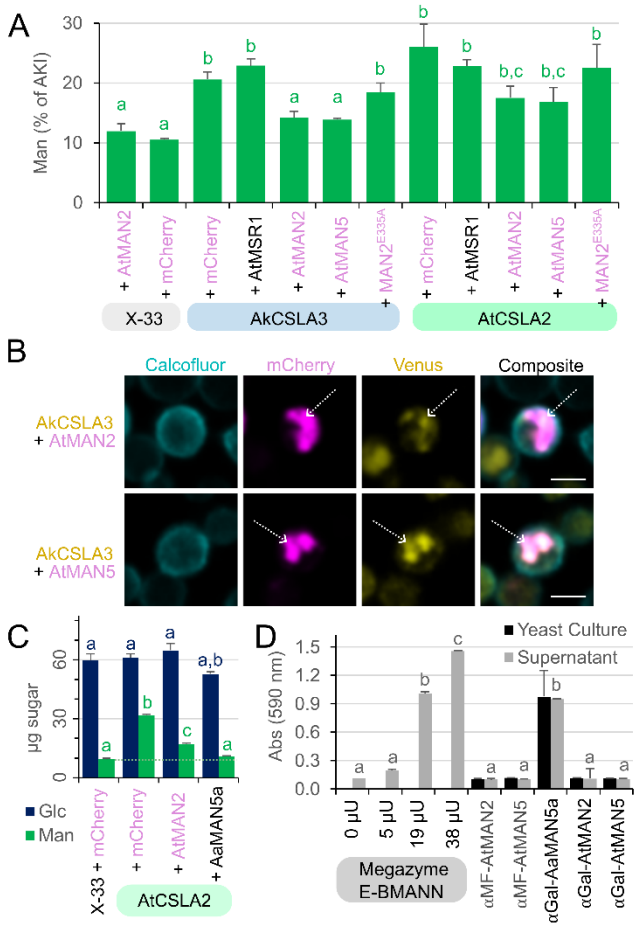


**Fig. 4.** Co-expression of *CSLA* and *MAN* in *Pichia* reduces insoluble β-mannan content. *(A)* AKI content of yeast cells. Bars show mean + SD of three biological replicates. *(B)* Arrows mark the co-localization of *AkCSLA3-Venus* and *AtMAN2/5-mCherry*. (Scale bars, 10 µm). *(C)* AKI composition of *AtCSLA2* strain co-expression with *AtMAN2 or* the microbial *AaMAN5a. (D)* AZCL-galactomannan digestion assays using *Saccharomyces* cell culture and supernatant. Dilute levels of a commercial MAN or AaMAN5a altered the absorbance at 590 nm, while *AtMANs* with either αMF or αGal signal peptides did not. For *(A)*, *(C)*, and *(D)*, different letters denote significant changes with one-way ANOVA (Tukey's post-hoc test, $P < 0.01$).

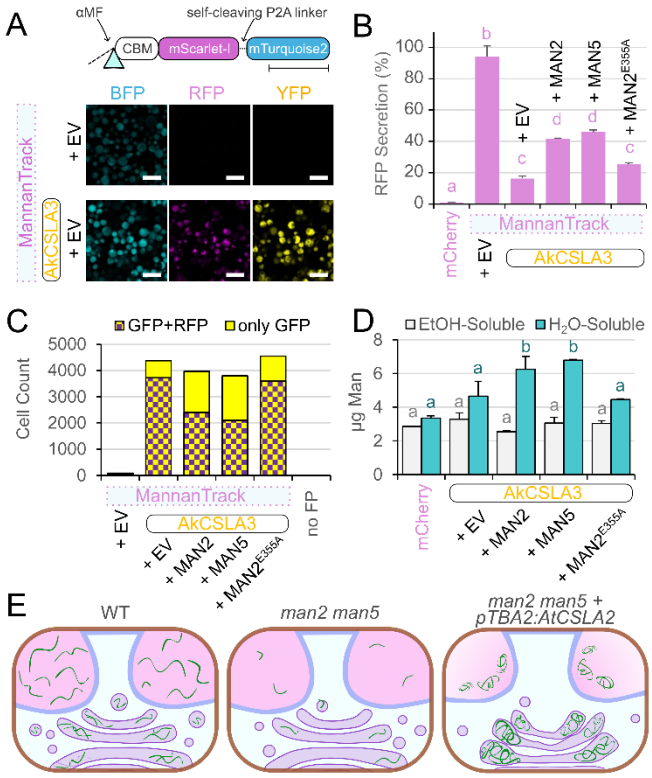


**Fig. 5.** *MAN2* and *MAN5* promote mannan secretion. *(A)* MannanTrack protein structure and confocal images of control strains. (Scale bars, 5 µm). *(B)* Percent red fluorescent protein (RFP) MannanTrack secretion from CSLA + MAN *Pichia* cells. Bars show mean + SD of three biological replicates. (*C)* Number of cells expressing GFP (for AkCSLA3-Venus) and RFP quantified via flow cytometry. *(D)* Monosaccharide content of Ethanol-soluble (EtOH-soluble) and hot water extract ($H_2O$-soluble) cells expressing AkCSLA3-Venus and MANs. Bars show mean + SD of three biological replicates. *(E)* Model for the beneficial roles of MAN2 and MAN5 on soluble mannan secretion to seed mucilage pockets. *(B)* and *(D)* Different letters denote significant changes with one-way ANOVA (Tukey's post-hoc test, $P < 0.01$).